Hydrothermal reaction of a rhyolitic-composition glass: A solid-state NMR study

Wang-Hong Alex Yang,* **R. James Kirkpatrick**

Department of Geology, University of Illinois, 1301 West Green St., Urbana, Illinois 61801, U.S.A.

Abstract

This paper presents a study of the structure and chemical composition of the solid products of the hydrothermal reaction of a synthetic Fe-free rhyolitic glass (Na_2O-K_2O-MgO-CaO-Al_2O_2-SiO_2) at 250 °C and nominally buffered pH of initially 1.0, 3.0, and 9.1 and of the mechanisms of this reaction using high-resolution solid-state NMR spectroscopy in combination with electron microprobe analysis, SEM, XRD, and IR spectroscopy. During this reaction molecular water is incorporated in the rhyolitic glass and substantially changes the glass's structure, as for a highly polymerized glass of nearly albite composition (Yang and Kirkpatrick, 1989). The structural changes due to hydration include an increased average Si-O-T (T = Si,Al) bond angle per tetrahedron and formation of hydration shells around the Na atoms and presumably around the other large cations. The three-dimensional aluminosilicate framework in the residual hydrated glass is not substantially depolymerized, the Si/Al ratio remains the same, and the dissolution of the aluminosilicate network occurs only at or near the glass-solution interface. The structural changes and the amount of dissolution are smaller than for the glass we previously examined, probably due to a higher Si/Al ratio and the presence of divalent cations as components of the rhyolitic composition. Additionally, the secondary minerals produced at high pH are clays rather than zeolites.

Introduction

Interaction between rhyolitic glass and aqueous fluids at low temperatures is a common process on and near the Earth's surface. The chemical changes in such glasses due to this process and the kinetics and mechanisms of this reaction have been previously studied (Jezek and Noble, 1978; Nesbitt and Young, 1984; White and Claassen, 1980 and references therein). There is also a large body of literature concerning leaching of glasses, especially potential nuclear waste storage materials (see Lutze, 1988, for a review). In many cases however, the structural changes in the glass due to aqueous attack and the nature and distribution of the solid reaction products are not well known. Understanding these factors is essential to clarifying the kinetics and mechanisms of such reactions.

In a previous paper (Yang and Kirkpatrick, 1989) we have shown that the dissolution of a nearly fully polymerized synthetic sodium aluminosilicate glass with a composition close to albite (NAS glass) at 250 °C in buffered aqueous solutions occurs by (1) incorporation of molecular water into bulk glass, (2) exchange of protons for Na, (3) a small amount of depolymerization in the interior of glass due to OH⁻ groups, and (4) dissolution of the aluminosilicate framework at the glass-water interface. The crystalline reaction products of these experiments become more polymerized with increasing pH,

and the average Si-O-T (T = Si,Al) bond angle per tetrahedron in the glass increases owing to the hydration. These conclusions are based on high-resolution solid-state nuclear magnetic resonance (NMR) spectroscopy in conjunction with X-ray diffraction (XRD), scanning electron microscopy (SEM), infrared spectroscopy (IR), and electron microprobe analysis.

In the study described here, we use the same techniques to analyze the solid products after a similar reaction between a synthetic, Fe-free rhyolitic glass (components Na_2O-K_2O-MgO-CaO-Al_2O_3-SiO_2) and hydrothermal fluids at 250 °C and nominally buffered pH of about 1.0, 3.0, and 9.1. Like the NAS glass, the rhyolitic glass is nearly fully polymerized (NBO/T = 0.07) but is closer to actual rock compositions. To avoid paramagnetic broadening of the NMR peaks, the glass was synthesized with no Fe. Ca and Mg were used to bring the total divalent cation content to about 6.5 mol%. The overall composition (Table 1) is similar to those of many natural rhyolites, except that it is deficient by ~1–2 wt% in total alkalis and similarly enriched in divalent cations (Carmichael et al., 1974).

Although the rhyolitic glass has a more complicated composition than the NAS glass, multinuclear (^{29}Si, ^{27}Al, ^{23}Na) magic-angle-spinning (MAS) and ^{29}Si and ^{27}Al cross-polarization magic-angle-spinning (CP-MAS) NMR spectroscopy is still a very sensitive probe of variations in structure and composition of the glass and the fine-grained, often amorphous, reaction products. The structural and compositional changes in the rhyolitic glass due

* Present address: EM Division, Geo-environmental Services, Inc., 130 West Wieuca Rd., Suite 108, Atlanta, Georgia 30342, U.S.A.

TABLE 1. Chemical analyses of the synthetic rhyolitic-composition glass used in this study

Component	As synthesized composition (wt%)	Analyzed average (wt%)*	Analyzed average (mol%)*
Na$_2$O	3.40	3.43	3.59
K$_2$O	3.50	3.55	2.44
MgO	2.50	2.68	2.69
CaO	3.10	3.37	3.89
Al$_2$O$_3$	14.10	14.63	9.30
SiO$_2$	73.40	72.44	78.10
Total	100.00	100.10	100.00
Si/Al (atomic)	4.42		4.20
NBO/T**			0.07

* Average of five electron microprobe analyses.
** Nonbridging O per tetrahedral cation.

to hydration are similar to those of the NAS glass. The rates of hydration and formation of secondary phases, however, are much smaller.

METHODS

The base glass was prepared by fusing reagent grade SiO$_2$, Al$_2$O$_3$, MgO, CaCO$_3$, K$_2$CO$_3$, and Na$_2$CO$_3$ mixtures in a Pt crucible at 1573 °C three times for about 40 min each time. The sample was quenched by immersing the bottom of the crucible in water and ground with an agate mortar and pestle between fusions. Composition and homogeneity were analyzed by using the methods described by Yang and Kirkpatrick (1989). Analyses could be taken to within about 5 μm of the edges of glass fragments. The nominal and analyzed compositions agree within analytical uncertainty (Table 1). The glass was ground and dry sieved to 5–40 μm for the hydrothermal experiments.

The hydrothermal experiments were carried out at 250 °C under autoclave conditions using the methods described by Yang and Kirkpatrick (1989). Solution pH was nominally buffered at 1.0 by 0.2 M KCl and 0.2 M HCl, at 3.0 by 0.1 M potassium hydrogen phthalate and 0.1 M HCl, and at 9.1 by 0.1 M (trihydroxylmethyl) aminomethane and 0.1 M HCl and changed to about 1.4, 5.2, and 9.4–9.8 (as measured at room temperature), respectively, during the experiments. Experiment times were up to 120 d. NMR, IR, XRD, and SEM data were obtained using the same methods as in our previous work. Some clay phases were separated from the experimental products using a sonifier and centrifuge and examined by powder XRD before and after expansion with ethylene glycol in an oriented mount on a ceramic tile using a Siemens powder diffractometer operated at 2° 2θ/min with Cu$K\alpha$ radiation.

RESULTS AND SPECTRAL INTERPRETATIONS

Base glass

The ^{29}Si, ^{27}Al, and ^{23}Na MAS NMR spectra of the base glass (dashed lines in Fig. 1) consist of single broad peaks. The ^{29}Si peak maximum is at -101.6 ppm and the

^{27}Al peak maximum is at 53.8 ppm at a magnetic field strength (H$_0$) of 11.7 T. Both are in the ranges for fully polymerized framework aluminosilicates (Kirkpatrick et al., 1985; Oestrike et al., 1987). There is no ^{27}Al peak due to octahedrally coordinated aluminum (Al[6]) which would occur at about 0 ppm. The ^{23}Na peak maximum is at -18.4 ppm at H$_0$ = 11.7 T, comparable to the value for the NAS glass. The broad peaks and the peak positions indicate that this glass, like glasses with similar compositions, has an essentially three-dimensional tetrahedral framework structure with a highly disordered Al-Si distribution and wide ranges of Si-O-T (T = Si,Al) bond angles (see, e.g., Hochella and Brown, 1984; Oestrike et al., 1987). Based on its composition and lack of Al[6], the method of Mysen et al. (1985), yields an average of 0.07 nonbridging O per tetrahedral cation (NBO/T), indicative of a nearly fully polymerized structure and consistent with the NMR data.

Hydrothermal reaction at pH 1.0 and 3.0

The reaction products of the rhyolitic glass are generally similar to those for the NAS glass, but the extent of the chemical and structural change is less. Even after 60 d at pH 1.0 (final pH = 1.4 at room temperature), powder XRD shows only a very broad hump with a maximum at about 24° 2θ, indicative of an amorphous aluminosilicate, and an almost unobservable peak at 12.3° 2θ corresponding to the 7.20 Å basal spacing of kaolinite. For the NAS glass, secondary phases were detected within 7 d. The presence of secondary kaolinite in the runs with the rhyolite glass is confirmed by the ^{27}Al MAS and ^{29}Si and ^{27}Al CP-MAS NMR data (Figs. 1B, 1E, and 2). The ^{27}Al MAS NMR spectra contain a small Al[6] peak at about 4 ppm corresponding to the Al[6] in kaolinite (Kinsey et al., 1985), in addition to that for Al[4] in residual glass. The relative intensity of the kaolinite Al[6] peak increases slowly with increasing experiment time. The relative intensity of this peak is much larger in the ^{27}Al CP-MAS NMR spectra (Figs. 2A, 2C), consistent with the high concentration of OH$^-$ groups in the kaolinite and our previous results for the NAS glass. The CP-MAS technique preferentially enhances the signal intensity from nuclei close to protons. The ^{29}Si MAS NMR spectrum of the 60-day sample (Fig. 1D) contains a small shoulder at about -91 ppm, corresponding to the Q^3(0Al) Si sites in kaolinite (Magi et al., 1981; Barron et al., 1983). The relative intensity of this signal is much larger in the ^{29}Si CP-MAS NMR spectra (-91.7 ppm peak in Figs. 2B, 2D).

SEM micrographs of the samples with pH 1 (e.g., Fig. 3A) show angular to slightly rounded fragments ~40 μm in size with an etched surface on which kaolinite (small white particles) appears to have precipitated. The size and morphology of the larger fragments indicate that they are residual glass, and thus that the amorphous phase detected by XRD and NMR is residual hydrated glass and not a new phase formed by dissolution and precipitation.
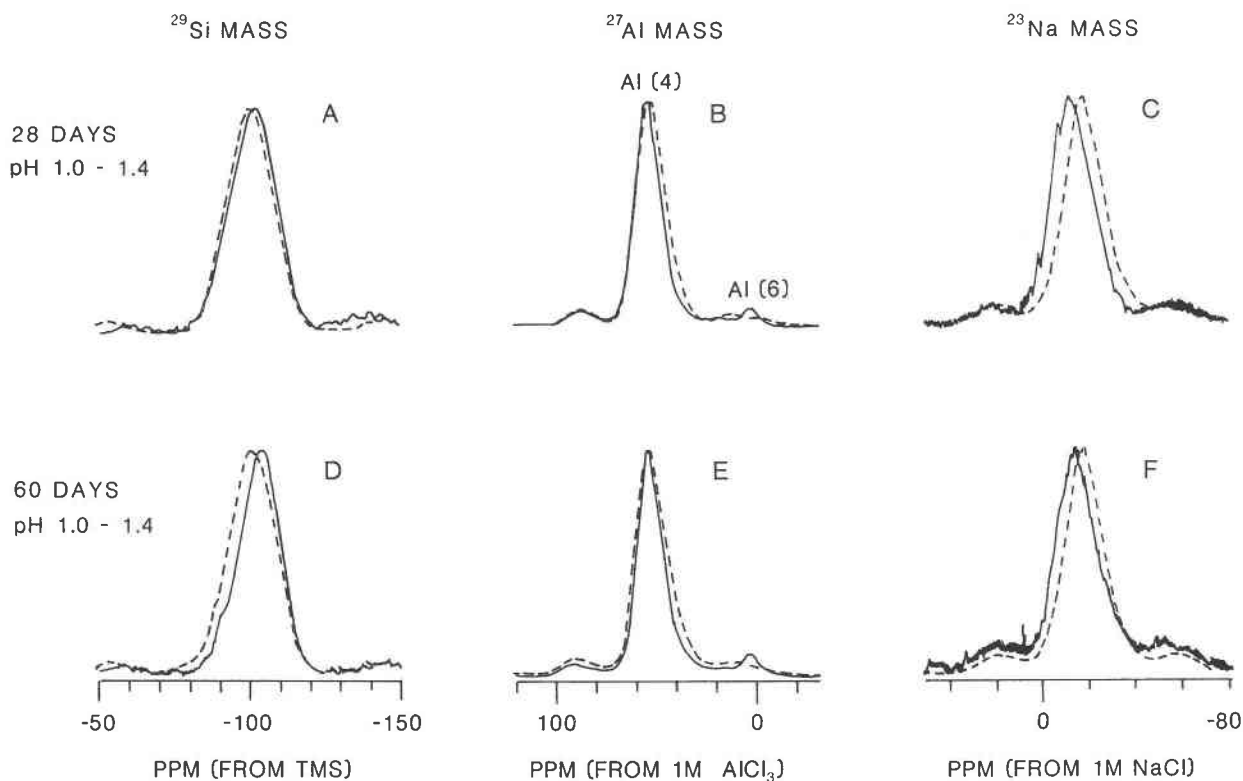
RHYOLITIC GLASS

Fig. 1. ^{29}Si (A, D), ^{27}Al (B, E), and ^{23}Na (C, F) MAS NMR spectra of rhyolitic glass after 28-d (A, B, C) and 60-d (D, E, F) hydrothermal reaction in buffered solution at pH 1.0 and 250 °C with a solution/solid ratio of 20 mL/g (final pH = 1.4). The dashed curves are the corresponding spectra of unreacted rhyolitic glass for comparison. The ^{29}Si spectra were collected at a magnetic field strength of 8.45 T, the ^{27}Al and ^{23}Na spectra at 11.7 T.

The ^{29}Si resonance of the residual glass becomes systematically narrower with increasing reaction time, from 17.0 ppm for the base glass to 15.3 ppm after 60 d. Simultaneously, the ^{29}Si peak maximum becomes more negative (shielded), from −101.6 ppm for the base glass to −104.9 ppm after 60 d (Figs. 1B, 1D). The position of the ^{27}Al[4] peak maximum does not change, but the peak becomes narrower, decreasing from 17.4 ppm for the base glass to 13.4 ppm after 60 d (Figs. 1B, 1E). The narrowing occurs on both sides of the peak, suggesting that it is caused at least in part by a decrease in the range of chemical shifts. A decrease in the average quadrupole coupling constant may also contribute to this peak narrowing. The ^{23}Na peak maximum becomes significantly less negative with reaction, from −18.4 ppm for the base glass to −13.8 ppm after 28 d and −15.1 ppm after 60 d. This change is not monotonic with increasing experiment time and is much less than the change from −19.0 ppm to −7.7 ppm observed for the NAS glass after 24 d. Unlike the reacted NAS glass, the ^{23}Na peak breadth for the rhyolitic glass does not become narrower with increasing reaction.

The IR spectra of the residual glass (not shown) are similar to those of reacted NAS glass and contain a broad X-O-H (X = H or a cation) stretching band at about 3500 cm^{-1} and an H-O-H bending band at about 1650 cm^{-1} (see, e.g., Newman et al., 1986). These results indicate that molecular H_2O or hydronium ion are important proton-bearing species (e.g., Ernsberger, 1977; Bartholomew et al., 1980).

In both the ^{29}Si and ^{27}Al CP-MAS NMR spectra, the intensity of the peaks due to hydrated glass increases relative to those due to kaolinite as the reaction proceeds (Fig. 2). There are also significant differences between the ^{27}Al and ^{29}Si MAS and CP-MAS NMR peak maxima (Fig. 2). The ^{29}Si CP-MAS resonance is less shielded than the corresponding MAS resonance, the difference increasing from 1.1 ppm at 28 d to 1.8 ppm at 60 d. The Al[4] ^{27}Al CP-MAS resonance due to hydrated glass is about 2.4 ppm less shielded than that of the corresponding MAS resonance after 60 d.

The compositional changes in the glass due to reaction are also similar to those in the NAS glass. With increasing reaction time at pH 1 the Si/Al ratio remains constant within analytical uncertainty, but the K content increases and Ca, Mg, and Na contents increase (Table 2), although
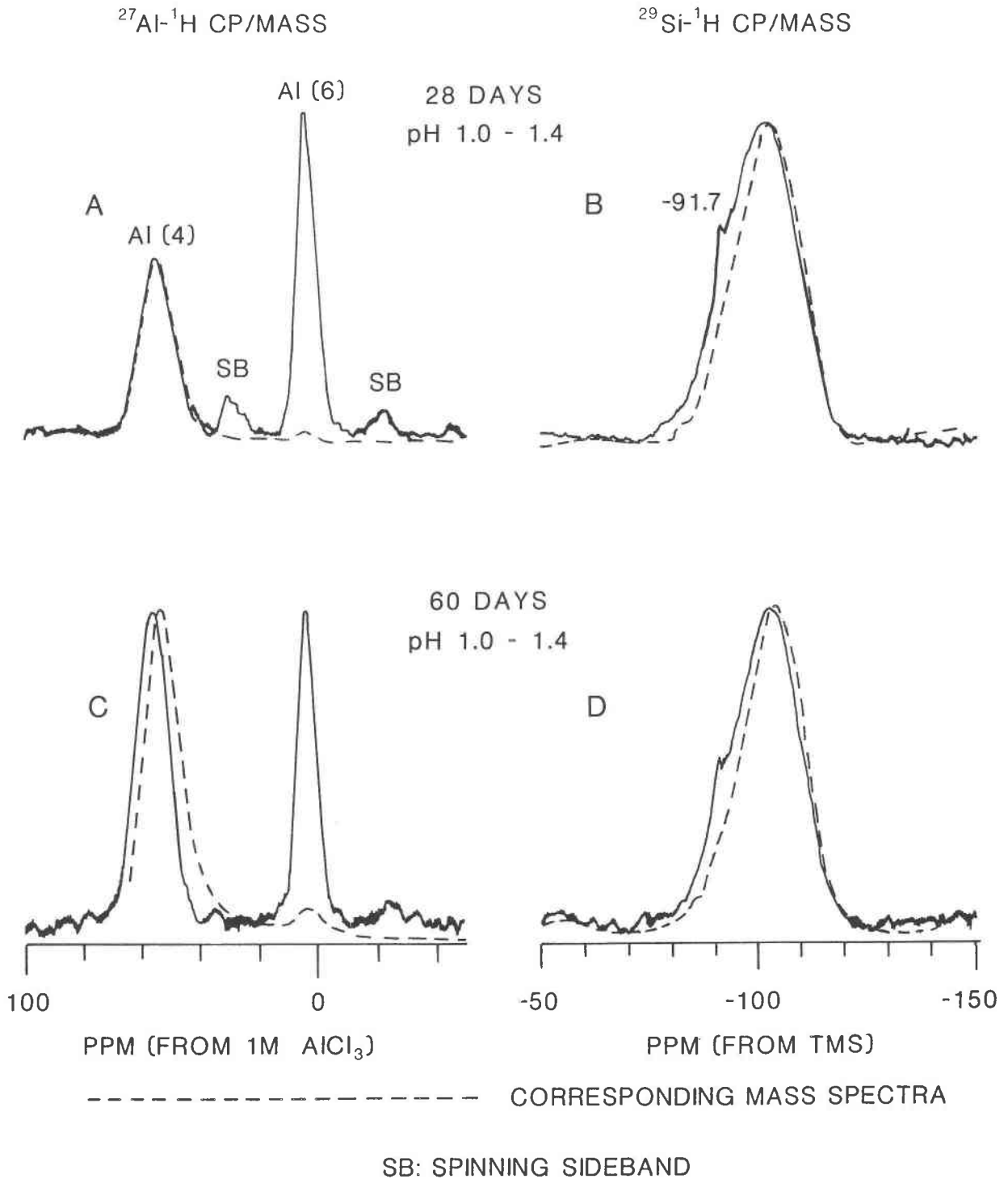
RHYOLITIC GLASS

Fig. 2. ^{27}Al-^{1}H (A, C) (800 μs contact time, 11.7 T) and ^{29}Si-^{1}H (B, D) (20 ms contact time, 8.45 T) CP-MAS NMR spectra of the rhyolitic glass after 28-d (A, B) and 60-d (C, D) hydrothermal reaction in buffered solution at pH 1.0 and 250 °C with a solution/solid ratio of 20 mL/g (final pH = 1.4). The dashed curves are the corresponding MAS NMR spectra of the same reacted samples for comparison.
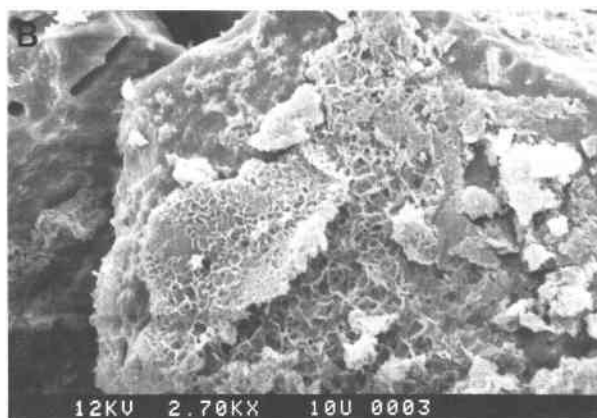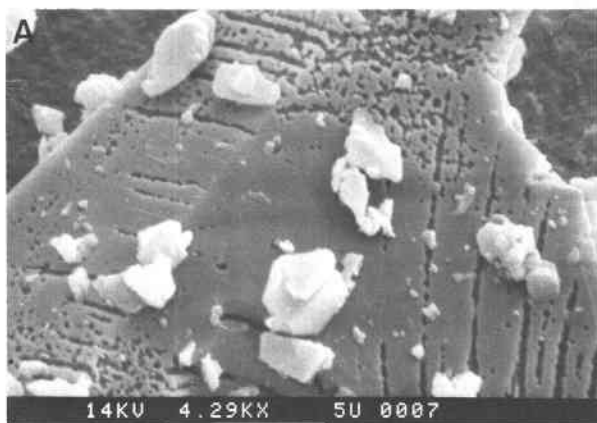
Fig. 3. (A) SEM micrograph of rhyolitic glass after 28-d hydrothermal reaction in buffered solution at pH 1.0 and 250 °C with a solution/solid ratio of 20 mL/g (final pH = 1.4). (B) SEM micrograph of the same glass after 60-d hydrothermal reaction in buffered solution at pH 9.1 and 250 °C with solution/solid ratio of 20 mL/g (final pH = 9.8).

TABLE 2. Comparison of chemical analyses of synthetic rhyolitic glass before and after hydrothermal reaction at 250 °C and for different pH values and experiment times

Component (wt%)	Un-reacted glass	pH 1.0–1.4* 28 d	pH 1.0–1.4* 60 d	pH 9.1–9.8* 60 d
Na₂O	3.43	3.18–3.74	0.13–3.08	1.24–3.65
K₂O	3.55	3.39–3.93	1.94–6.24	2.59–4.14
MgO	2.68	2.06–2.65	1.63–2.89	1.78–2.46
CaO	3.37	2.46–3.28	1.86–3.52	1.95–3.10
Al₂O₃	14.63	12.59–14.61	11.06–14.29	11.10–14.43
SiO₂	72.44	70.38–71.82	65.75–71.89	67.84–71.16
TOTAL	100.10	95.88–98.16	90.01–95.80	88.83–96.96
H₂O**	0.0	1.9–4.2	4.3–10.1	3.1–11.3
Si/Al (atomic)	4.20	4.11–4.84	3.90–4.81	4.14–4.86

* Range given is total range for all electron microprobe analyses.
** Difference between 100.10% and analyzed total.

more slowly than the Na content of the NAS glass decreases. The increased K content is probably due to K uptake from the KCl-HCl buffered solution. The maximum proton content of the reacted glass, as estimated by low totals in the microprobe analyses (Jezek and Noble, 1978) is about 10–11 wt% as H_2O, comparable to the maximum content for the reacted NAS glass. The distribution of the protons within the glass is difficult to determine because of the small grain size.

The reaction between rhyolitic glass and pH 3.0 buffered solution was extremely slow, and the spectral changes are similar to those at pH 1.0 (data not shown). This result is consistent with the results for the NAS glass.

Hydrothermal reaction at pH 9.1

The reaction of the rhyolitic glass at pH 9.1 occurred slowly also, and even after 120 d there were many residual glass fragments readily observed by SEM (e.g., Fig. 3B). This observation contrasts with the results of the

NAS glass, which reacted substantially at high pH after only 7 d. For the rhyolite glass, powder XRD of non-oriented samples shows a very broad peak with a maximum at about 24° 2θ, corresponding to the residual glass, and a broad peak with a maximum at about 6.50° 2θ, which corresponds to a typical $d(001)$ of smectite.

Powder XRD patterns of separated and oriented samples of this layer silicate contain low-angle peaks with $d(001)$ values of 15.11 Å (60-day sample) and 14.42 Å (120-day sample). These $d(001)$ spacings expand to 17.7 Å and 17.0 Å, respectively, after treatment with ethylene glycol. This clay is, thus, an expandable smectite.

The presence of smectite is confirmed by the NMR data (Figs. 4 and 5) and SEM observation (Fig. 3B). It is represented by the ²⁹Si NMR peak at −94.5 ppm (Figs. 4A, 4D; Weiss et al., 1987) and the ²⁷Al NMR peak for Al[6] at about 4 ppm (Figs. 4B, 4E). The ²⁷Al signal for the clay, including a shoulder for Al[4] at about +68.2 ppm (Kinsey et al., 1985), is preferentially enhanced in the ²⁷Al CP-MAS NMR spectra due to its large OH content (Figs. 5A, 5C). The ²⁷Al shoulder at 68.2 ppm indicates some Al for Si substitution in the tetrahedral sheet of the smectite (Kinsey et al., 1985). The ²⁹Si and ²⁷Al peak maxima for this clay are more shielded than those of the smectite formed by reaction of the NAS glass with buffered solutions with pH 3.0–5.5. This difference is probably due to a significant amount of Mg[6] in the clay formed from the rhyolitic glass (Weiss et al., 1987). Thus, this clay is probably a trioctahedral smectite, such as saponite, containing some Al[6]. Both XRD and NMR indicate that the fraction of the smectite increases with increasing experiment time. There is no NMR, XRD, or SEM evidence for the presence of zeolites in these samples, as was observed for the NAS glass reacted at pH 9.1.

The NMR spectra and electron microprobe data of the pH 9.1 samples (Figs. 4 and 5) also indicate structural and compositional changes in the residual glass due to hydrothermal reaction. The ²⁹Si peak maximum becomes slightly more negative, changing from −101.6 ppm for unreacted glass to −103.4 ppm after 60 d and −103.8
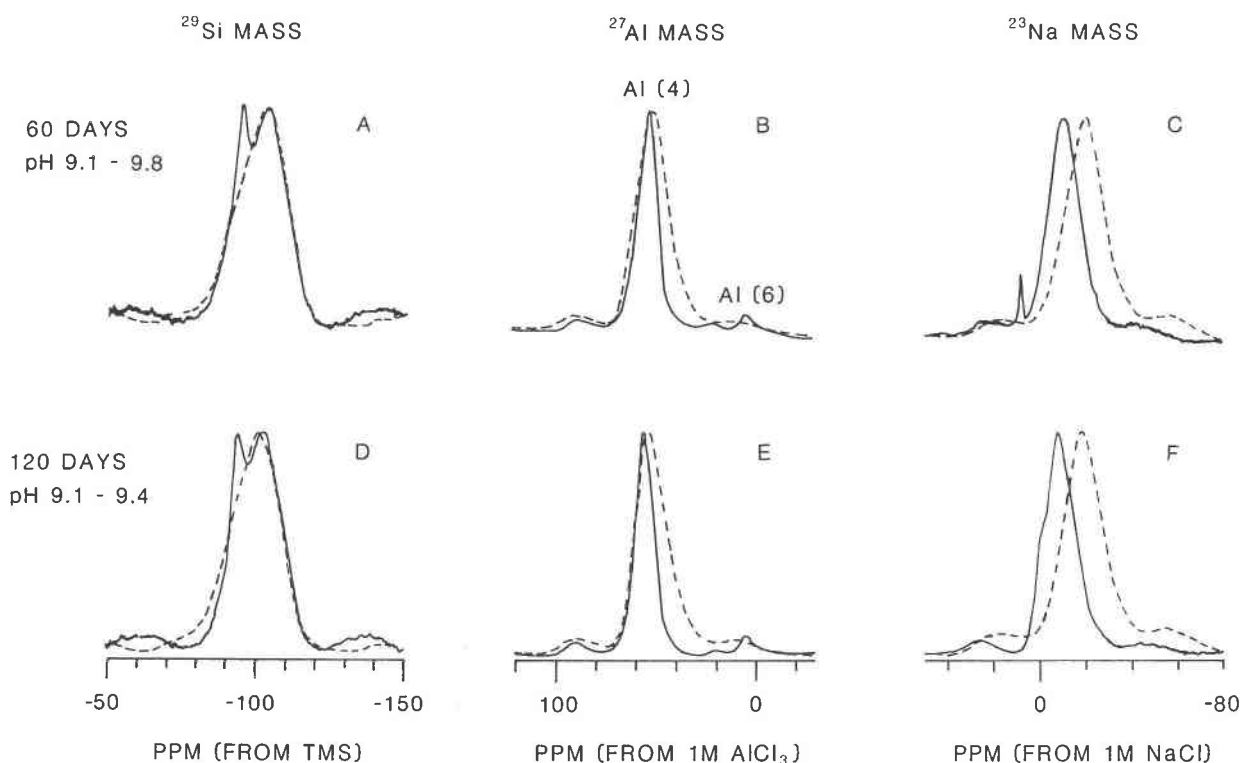
Fig. 4. ^{29}Si (**A, D**), ^{27}Al (**B, E**), and ^{23}Na (**C, F**) MAS NMR spectra of rhyolitic glass after 60-d (A, B, C) and 120-d (D, E, F) hydrothermal reactions in a buffered solution with initial pH of 9.1 at 250 °C with a solution/solid ratio of 20 mL/g (final pH = 9.8). The dashed curves are the corresponding NMR spectra of unreacted rhyolitic glass for comparison. Spectral condition as in Figure 1.

ppm after 120 d. This change is slightly smaller than at low pH for the same run time. The ^{29}Si, ^{27}Al, and ^{23}Na NMR peaks for the residual rhyolitic glass at pH 9.1 become systematically narrower with increasing experiment time. The maximum H_2O content at pH 9.1 is about 10 wt% (Table 2), comparable to the pH 1 results. The IR spectra of the experimental products (not shown) are similar to those of the pH 1 samples and contain X-O-H (X = H or a cation) stretching and H-O-H bending bands.

The ^{27}Al and ^{29}Si CP-MAS NMR peak positions for the residual glass after 120 d at pH 9.1, however, are only about 0.3 ppm less shielded than the corresponding MAS peaks, a significantly smaller difference than at pH 1. The ^{29}Si CP-MAS peak maximum for the 120-d experiment becomes more shielded with increasing Hartmann-Hahn contact time (Hartmann and Hahn, 1962; Fig. 6). The Hartmann-Hahn contact time is the time during which the spin systems of ^{1}H and the second nuclide (e.g., ^{27}Al or ^{29}Si) are simultaneously excited and can exchange nuclear spin (see Yannoni, 1982, for an introduction to the CP-MAS method).

The ^{23}Na peak maximum becomes significantly less negative, from −18.4 ppm for the base glass to −9.1 ppm

after 60 d and to −8.4 ppm after 120 d. The peak width also decreases from 18.6 ppm for unreacted glass to 14.8 ppm after 60 d and 15.2 ppm after 120 d. These changes are significantly larger than for the experiments with pH 1.0–1.4.

As at pH 1.0, the Si/Al ratio of the glass remains constant and the same as that of the base glass. Less Na-, Ca-, and Mg-leaching and K-uptake occur under alkaline conditions than under acid conditions after similar experiment times (Table 2).

DISCUSSION

Proton speciation

The results described here demonstrate that the structural and compositional changes in the rhyolitic glass due to proton uptake are similar to those in the NAS glass. The NMR, XDR, and SEM data (Fig. 3) show that hydrated glass is the major reaction product at all pH values. The size, morphology, and etched or ripplelike features on the surfaces of the reacted fragments indicate that they are residual glass rather than a secondary amorphous phase formed by dissolution and precipitation. Both
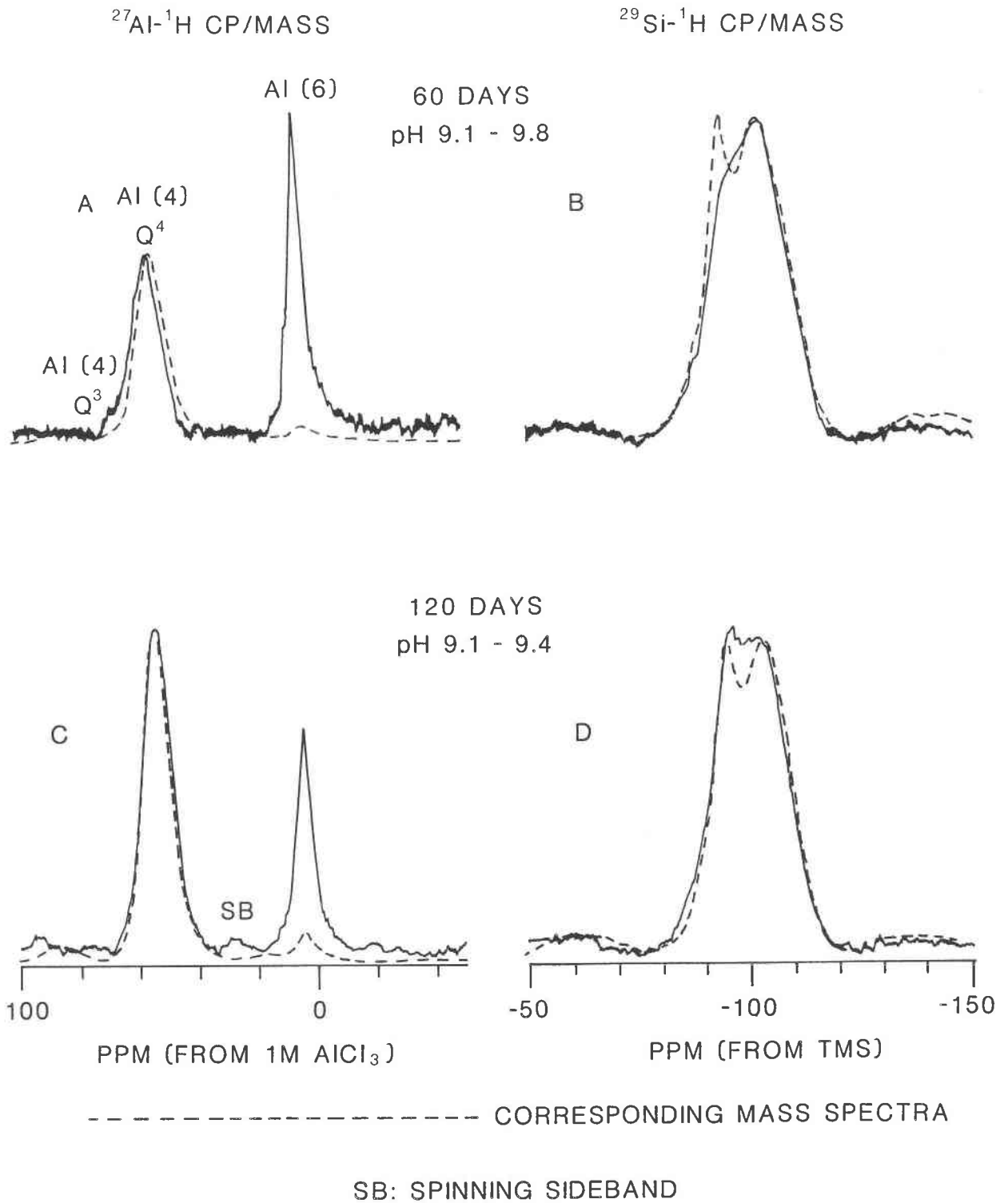
RHYOLITIC GLASS

^{27}Al-^{1}H CP/MASS

^{29}Si-^{1}H CP/MASS

Al (6)

60 DAYS
pH 9.1 - 9.8

A   Al (4)
Q^4

B

Al (4)
Q^3

120 DAYS
pH 9.1 - 9.4

C

SB

D

100   0

PPM (FROM 1M AlCl$_3$)

-50   -100   -150

PPM (FROM TMS)

– – – – – – – – – – – – CORRESPONDING MASS SPECTRA

SB: SPINNING SIDEBAND

Fig. 5. ^{27}Al-^{1}H (**A, C**) (800 μs contact time, 11.7 T) and ^{29}Si-^{1}H (**B, D**) (20 ms contact time for B and 2 ms contact time for D, 8.45 T) CP-MAS NMR spectra of rhyolitic glass after 60-d (A, B) and 120-d (C, D) hydrothermal reaction in a buffered solution initially at pH 9.1 and at 250 °C with a solution/solid ratio of 20 mL/g (final pH = 9.8). The dashed curves are the corresponding MAS NMR spectra of the same reacted samples for comparison.
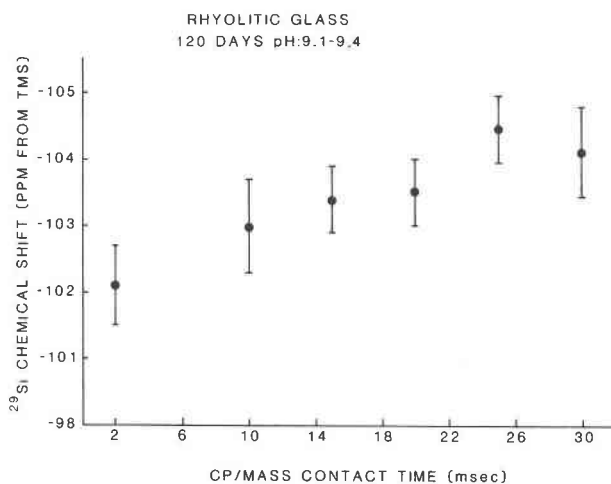
Fig. 6. Chemical shift (peak maximum) in the ^{29}Si CP-MAS NMR spectra (8.45 T) of hydrated rhyolitic glass after 120-d hydrothermal reaction in pH 9.1 solution vs. the Hartmann-Hahn contact time (Hartmann and Hahn, 1962) used in the CP-MAS experiment. The increased shielding with increasing contact time is consistent with the presence of Si-O-H linkages, because these linkages have shorter Si-H distances and more deshielded chemical shifts than Q^4Si atoms in tetrahedra with H_2O molecules. The short contact time thus preferentially enhances the Si sites having shorter Si-H distances.

^{27}Al and ^{29}Si in this residual glass readily cross-polarize, consistent with the electron microprobe results that indicate proton contents of up to about 10 wt% as H_2O.

The relatively shielded ^{27}Al[4] and ^{29}Si MAS NMR chemical shifts of the residual glass (Figs. 1 and 4) indicate that it remains highly polymerized after hydration and that not many protons are present as OH$^-$ groups. The large H-O-H bending band at 1650 cm^{-1} in the IR spectra (not shown) also indicates the presence of molecular H_2O or hydronium ion. Using the microprobe analyses of Table 2 and the methods of Yang and Kirkpatrick (1989), the maximum number of OH$^-$ groups per tetrahedron required for charge balance is zero within analytical uncertainty at both pH 1 and 9. Clearly, the dominant proton-bearing species in the hydrated glass at these pH values is molecular H_2O, as it is for the NAS glass.

The increasing deshielding at ^{29}Si and ^{27}Al in the CP-MAS NMR spectra relative to the corresponding MAS NMR spectra with increasing experiment time, especially at pH 1, however, suggests that a small number of OH$^-$ groups on Si tetrahedra are present and that their concentration increases with increasing experiment time. Si tetrahedra with one attached OH$^-$ group (Q^3-OH sites) typically resonate at chemical shifts about 10 ppm less shielded than those with no OH groups (e.g., Brinker et al., 1988; Farnan et al., 1987). This signal from the Q^3-OH sites is preferentially enhanced under CP-MAS conditions, causing the observed decreased shielding.

The increased shielding of the peak maxima in the ^{29}Si

CP-MAS spectra with increasing Hartmann-Hahn contact time (Fig. 6) is also consistent with the presence of some OH$^-$ groups attached to Si tetrahedra. Farnan et al. (1987) have shown that for hydrous SiO_2 glasses, the relative intensity of the Q^3-OH sites decreases with increasing contact time, because longer contact times allow Si nuclei farther from the protons to be polarized. For our glasses, separate ^{29}Si peaks cannot be resolved because of Si/Al and bond-angle disorder, and the effect of such a relative decrease in intensity for Si on Q^3-OH sites would be an increase in the average shielding, as observed. The number of OH$^-$ groups necessary to cause the chemical shift differences between the MAS and CP-MAS spectra could be quite low, because OH$^-$ groups could be much more efficient at cross-polarizing Si than H_2O molecules, especially if the H_2O molecules are in rapid motion.

Natural hydrated rhyolitic glasses (perlite, pitchstone, etc.) typically contain 2–10 wt% meteoritic water (Ross and Smith, 1955; Friedman and Smith, 1958; Jezek and Noble, 1978 and references therein). Obsidian can even absorb H_2O from the atmosphere to form a hydrated layer (Friedman and Long, 1976). The results of this study suggest that the protons in natural rhyolitic glass are probably present mostly as molecular H_2O. H_2O-bearing albitic, rhyolitic, and basaltic glasses quenched from above the liquidus contain coexisting molecular H_2O and OH groups with the relative amount of H_2O molecules increasing with increasing H_2O content (Stolper, 1982). Farnan et al. (1987) found a similar result for SiO_2 glasses.

It is also possible that the residual glass is heterogeneous, with volumes with lower Si/Si + Al ratios (less shielded ^{29}Si chemical shifts) giving rise to more intense signals in the CP spectra. We see no evidence to support this possibility.

Structural variations due to hydration

The changes in the ^{23}Na, ^{27}Al, and ^{29}Si NMR peak maxima and widths (Figs. 1 and 4) indicate considerable structural change in the rhyolitic glass after reaction. As for the NAS glass, these variations appear to be related to leaching of large cations from the glass (in this case Na$^+$, Mg^{2+}, Ca^{2+}) and uptake of proton-containing species and to a lesser extent K$^+$ from the buffered solution. The Si/Al ratio remains essentially constant (Table 2).

The ^{29}Si peak maxima of the residual glasses become more shielded with increasing experiment time. Because the Si/Al ratio remains constant, this increased shielding at ^{29}Si is most likely due to an increased average Si-O-T (T = Si,Al) bond angle per tetrahedron (Radeglia and Engelhardt, 1985 and references therein). Based on the correlation of Smith (1984), the average Si-O-T bond angle per tetrahedron increases from about 145° for the unreacted glass to about 148° for the most shielded hydrated sample. These bond-angle changes are probably caused by a decrease in the cation-induced polarization of the Si-O bonds due to a hydration shell of molecular H_2O

around the large cations and to cation-leaching (Yang and Kirkpatrick, 1989).

Another significant change in the NMR spectra is that the ^{29}Si and ^{27}Al peak widths of the residual glass become narrower with increasing hydration (Figs. 1 and 4). This decrease in peak width indicates that as the Si-O-T bond angles increase owing to hydration, the range of average Si-O-T bond angle per tetrahedron decreases. The decreased shielding and possibly more isotropic environment at ^{23}Na with increasing H_2O content are probably due to the formation of a shell of H_2O molecules around the Na cations. The average number of H_2O molecules per large cation estimated from microprobe analyses and the method of Yang and Kirkpatrick (1989) are 0.54 ($\pm \sim 0.2$) after 28 d and 2.53 ($\pm \sim 0.2$) after 60 d at pH 1.0–1.4, and 2.16 ($\pm \sim 0.3$) after 60 d at pH 9.1–9.8. This hydration reduces the interaction between the Na-cations and the O of the aluminosilicate framework. However, at pH 1 the ^{23}Na peak width does not narrow monotonically with increasing H_2O content or as much as for the NAS glass. These differences are probably due to the presence of some unhydrated Na atoms, possibly because of competition for the H_2O molecules by other larger cations, such as Ca^{2+} and Mg^{2+}, which have larger hydration energies. This reason and the smaller average number of H_2O molecules per large cation probably account for the smaller changes in the ^{23}Na NMR parameters of the rhyolitic glass relative to the NAS glass.

The ^{23}Na peaks for the hydrated rhyolite glass at pH 9.1–9.8 after 60 d are narrower and more shifted compared to those of the base glass than those for the glass at pH 1.0–1.4 after 60 d, despite a similar average number of H_2O molecules per large cation. This difference is probably due to the smaller amount of cation-exchange under alkaline conditions (Table 2). At pH 1.0–1.4 most of the Na-atoms accessible to molecular H_2O are likely to be leached and, thus, a larger fraction of the Na atoms are unhydrated or have incomplete hydration shells. At pH 9.1, less Na is leached (Table 2), and it remains in the glass to be hydrated. Thus, the ^{23}Na NMR spectra of the pH 1.0 glasses are more like those of the base glass than those of the glasses at pH 9.1. This slower leaching at higher pH is similar to the results for many borosilicate nuclear waste glasses (see Lutze, 1988, for a review).

Although the changes in peak position and width in the ^{23}Na, ^{27}Al, and ^{29}Si NMR peaks of the rhyolitic glass due to hydration are similar to those for the NAS glass, the extent of the variation for the rhyolitic glass is much smaller. Cation exchange and incorporation of H_2O molecules over tens of micrometers without disruption of the aluminosilicate network of the glass must occur by solid-state diffusion. Thus, the slower reaction rate for the rhyolitic glass is due to lower exchange diffusion coefficients. This slower diffusion is probably caused by a higher Si/Al ratio and the presence of divalent cations, which have smaller diffusion coefficients in framework aluminosilicate glasses (Winchell, 1969).

The mechanism of glass dissolution

The SEM evidence for residual glass fragments and dissolution features on the glass surface, the microprobe evidence of substantial cation exchange at apparently constant Si/Al, and the NMR evidence of internal structural changes in the glass indicate that the dissolution of the rhyolite glass is incongruent and involves diffusion-controlled cation exchange in the interior of the glass and disruption of the aluminosilicate network at the glass-water interface. The rate of cation exchange is greater at pH 1.0 than at pH 9.1 (Table 2). This difference may be related to the ratio of the activities of alkali cations to protons in solution, with the low ratio of low pH causing more rapid cation exchange. White and Claassen (1980) have shown that mass-transfer rate constants for Na^+, Mg^{2+}, and Ca^{2+} during dissolution of a rhyolitic glass decrease with increasing pH, consistent with this idea.

The XRD, SEM, and NMR data indicate that the rate of formation of secondary phases at pH 9.1 is more rapid than at pH 1.0. This higher rate reflects more rapid disruption of the aluminosilicate framework at pH 9.1. The high OH^- concentration in alkaline solutions accelerates the aqueous attack on the aluminosilicate network near or on the glass surface by nucleophilic attack of Si tetrahedra (Iler, 1976; Bunker et al., 1988).

The dissolution mechanism of the rhyolitic glass thus consists of the following simultaneous steps: incorporation of molecular H_2O into the glass, exchange of protons and large cations between the glass and fluid, a small amount of depolymerization of the aluminosilicate framework in the interior of the glass, and disruption of the aluminosilicate framework at the glass-H_2O interface. Cation exchange is relatively less important at high pH values.

Secondary phases

The secondary crystalline phases formed from the rhyolitic glass are kaolinite at pH 1.0–1.4 and smectite, probably saponite, at pH 9.1–9.8. As shown in the SEM micrographs (Fig. 3), these clay phases precipitate on the surface of the residual glass and thus the reaction occurs by dissolution and precipitation. The lack of secondary zeolites at high pH is probably due to the presence of Mg leached from the glass. Hawkins and Roy (1963) have shown that smectite rather than a zeolite is the chief reaction product formed from Mg-bearing solutions. Thus, we expect that the products of natural rhyolite-H_2O reaction should depend on the MgO content of the initial glass and the relative efficiency with which Mg is removed from the local system, as well as the local physical and chemical conditions.

CONCLUSIONS

The dissolution of a synthetic rhyolitic glass at 250 °C under autoclave conditions and initial buffered pH values of 1.0, 3.5, and 9.1 occurs incongruently, with incorpo-

ration of molecular H_2O, a small amount of depolymerization of the aluminosilicate framework probably due to OH^- groups, cation exchange throughout the glass fragments, and dissolution of the aluminosilicate framework at the glass-H_2O interface. These results are similar to those for the sodium aluminosilicate glass examined by Yang and Kirkpatrick (1989). The proton-bearing species, almost entirely molecular H_2O, are eventually incorporated throughout the glass and change its structure. The structural changes caused by this hydration include larger average Si-O-T (T = Si,Al) bond angles per Si-tetrahedron and narrower ranges of ^{29}Si, ^{27}Al, and ^{23}Na chemical environments. At both pH 1.0 and 9.1, the three-dimensional framework of the glass is not substantially depolymerized and its Si/Al ratio remains the same. The less shielded ^{23}Na environments in the hydrated glasses are likely caused by the formation of a shell of H_2O molecules around the Na atoms in the residual glass, reducing their bonding interaction to the bridging O. The Na atoms in the residual glass at pH 9.1–9.8 are more hydrated than those at pH 1.0–1.4 after the same experiment time, probably owing to more rapid leaching of hydrated Na under acid conditions.

The rates of structural change and dissolution of the rhyolitic glass due to aqueous attack are slower than for the sodium aluminosilicate glass. This difference is probably related to the presence of divalent cations in the rhyolitic glass and its higher Si/Al ratio. Divalent cations have smaller diffusion coefficients than monovalent cations and also apparently cause reduction in the mass-transfer rate of Na^+ and K^+ (Winchell, 1969; White and Claassen, 1980).

The secondary phases precipitated from solution are kaolinite at pH 1.0–1.4 and an expandable 2:1 layer phyllosilicate, probably saponite, at pH 9.1–9.8. Unlike the results for the sodium aluminosilicate glass, no zeolites form at pH 9.1–9.8, probably because of the presence of Mg in the system.

ACKNOWLEDGMENTS

REFERENCES CITED

Barron, P.F., Frost, R.L., Skjenitad, J.O., and Koppi, A.J. (1983) Detection of two silicon environments in kaolins by solid state 29Si NMR. Nature, 299, 616–618.

Bartholomew, R.F., Butler, B.L., Hoover, H.L., and Wu, C.K. (1980) Infrared spectra of a water-containing glass. Journal of the American Ceramic Society, 63, 481–485.

Brinker, C.J., Kirkpatrick, R.J., Tallant, D.R., Bunker, B.C., and Montez, B. (1988) NMR confirmation of strained "defects" in amorphous silica. Journal of Non-Crystalline Solids, 99, 418–428.

Bunker, B.C., Tallant, D.R., Headley, J.J., Turner, G.L., and Kirkpatrick, R.J. (1988) The structure of leached sodium borosilicate glass. Physics and Chemistry of Glasses, 29, 106–120.

Carmichael, I.S.E., Turner, F.J., and Verhoogen, J. (1974) Igneous Petrology, 739 p. McGraw-Hill, New York.

Ernsberger, F.M. (1977) Molecular water in glass. Journal of the American Ceramic Society, 60, 91–92.

Farnan, I., Kohn, S.C., and Dupree, R. (1987) A study of the structural role of water in hydrous silica glass using cross-polarization magic angle spinning NMR. Geochimica et Cosmochimica Acta, 51, 2869–2873.

Friedman, I., and Long, W. (1976) Hydration rate of obsidian: New experimental techniques allow more precise dating of archeological and geological sites containing obsidian. Science, 191, 347–352.

Friedman, I., and Smith, R.L. (1958) The deuterium content of water in some volcanic glasses. Geochimica et Cosmochimica Acta, 15, 218–228.

Hartmann, S.R., and Hahn, E.L. (1962) Nuclear double resonance in the rotating frame. Physical Review, 128, 2042–2053.

Hawkins, D.B., and Roy, R. (1963) Distribution of trace elements between clays and zeolites formed by hydrothermal alteration of synthetic basalts. Geochimica et Cosmochimica Acta, 27, 785–795.

Hochella, M.F., Jr., and Brown, G.E., Jr. (1984) Structure and viscosity of rhyolitic composition melts. Geochimica et Cosmochimica Acta, 48, 2631–2640.

Iler, R.K. (1976) The chemistry of silica. Wiley, New York.

Jezek, P.A., and Noble, D.C. (1978) Natural hydration and ion exchange of obsidian: An electron microprobe study. American Mineralogist, 63, 266–273.

Kinsey, R.A., Kirkpatrick, R.J., Hower, J., Smith, K.A., and Oldfield, E. (1985) High resolution aluminum-27 and silicon-29 nuclear magnetic resonance spectroscopic study of layer silicates, including clay minerals. American Mineralogist, 70, 537–548.

Kirkpatrick, R.J., Kinsey, R.A., Smith, K.A., Henderson, D.M., and Oldfield, E. (1985) High resolution solid state sodium-23, aluminum-27, and silicon-29 nuclear magnetic resonance spectroscopic reconnaissance of alkali and plagioclase feldspars. American Mineralogist, 70, 106–123.

Lutze, W. (1988) Silicate glasses. In W. Lutze and R.C. Ewing, Eds., Radioactive waste forms for the future, p. 3–159. North-Holland Publishing, Amsterdam.

Magi, M., Samoson, A., Tarmak, M., Engelhardt, G., and Lippmaa, E. (1981) Studies of the structure of silicates and zeolites by solid-state high-resolution silicon-29 NMR spectroscopy. Doklady Akademii Nauk SSSR Novaia Seriia, 261, 1169–1174 (in Russian).

Mysen, B.O., Virgo, D., and Seifert, F.A. (1985) Relationships between properties and structure of aluminosilicate melts. American Mineralogist, 70, 88–105.

Nesbitt, H.W., and Young, G.M. (1984) Prediction of some weathering trends of plutonic and volcanic rocks based on thermodynamic and kinetic considerations. Geochimica et Cosmochimica Acta 48, 1523–1534.

Newman, S., Stolper, E.M., and Epstein, S. (1986) Measurement of water in rhyolitic glasses: Calibration of an infrared spectroscopic technique. American Mineralogist, 71, 1527–1541.

Oestrike, R., Yang, W.-H., Kirkpatrick, R.J., Hervig, R.L., and Navrotsky, A. (1987) High-resolution ^{23}Na, ^{27}Al, and ^{29}Si NMR spectroscopy of framework silicate glasses. Geochimica et Cosmochimica Acta, 51, 2199–2209.

Radeglia, R., and Engelhardt, G. (1985) Correlation of Si-O-T (T = Si or Al) angles and ^{29}Si chemical shifts in silicates and alumino-silicates: Interpretation by semi-empirical quantum-chemical considerations. Chemical Physics Letters, 114, 28–30.

Ross, C.S., and Smith, R.L. (1955) Waters and other volatiles in volcanic glasses. American Mineralogist, 40, 1071–1089.

Smith, K.A. (1984) High-resolution solid-state silicon-29 nuclear magnetic resonance studies of minerals and glasses. Ph.D. thesis, University of Illinois, Urbana.

Stolper, E. (1982) Water in silicate glasses: An infrared spectroscopic study. Contributions to Mineralogy and Petrology, 81, 1–17.

Weiss, C.A., Altaner, S.P., and Kirkpatrick, R.J. (1987) High resolution ^{29}Si NMR spectroscopy of 2:1 layer silicates, correlations among chemical shift, structural distortion, and chemical variations. American Mineralogist, 72, 935–942.

White, A.F., and Claassen, H.C. (1980) Kinetic model for the short-term dissolution of a rhyolitic glass. Chemical Geology, 28, 91–109.

Winchell, P. (1969) The compensation law for diffusion in silicates. High Temperature Science, 1, 200–215.

Yang, W.-H.A., and Kirkpatrick, R.J. (1989) Hydrothermal reaction of albite and a sodium aluminosilicate glass: A solid-state NMR study. Geochimica et Cosmochimica Acta, 53, 805–819.

Yannoni, C.S. (1982) High-resolution NMR in solids: The CPMAS experiment. Accounts of Chemical Research, 15, 201–208.